Reversibility and isotope effect of the calorimetric glass → liquid transition of low-density amorphous ice

Michael S. Elsaesser,[a] Katrin Winkel,[ab] Erwin Mayer[b] and Thomas Loerting*[a]

We here report differential scanning calorimetry (DSC) scans recorded by repeatedly heating the H_2O (D_2O) low density amorph (LDA) which was made by isothermal decompression of very high-density amorphous ice (VHDA) at 140 K from 1.1 to 0.006 GPa. These DSC scans show a glass → liquid transition endotherm with an onset temperature (T_g) of ≈ 137 (140) K at a heating rate of 30 K min^{-1} accompanied by an increase in heat capacity of ≈ 1.7 (1.5) J K^{-1} mol^{-1}. We establish the reversibility of this effect by thermally cycling between its glassy state below 137 K and its highly viscous liquid state at 149 K. All calorimetric signatures, including H/D isotope effect, are highly similar to the signatures in hyperquenched glassy water (HGW). We argue that the observation of almost identical calorimetric traces for HGW and LDA implies that there is no need to reassign HGWs T_g to higher temperatures provided that the viscous liquid state connected to both LDA and HGW behaves as an ideally "strong" liquid in the Angell classification. We furthermore show that LDA prepared by isothermal decompression of VHDA is more crystallization-resistant than LDA made from high-density amorphous ice (HDA) by isobaric warming. We suggest that the former route *via* VHDA removes "nanocrystalline remnants" in LDA which are still present in the latter after pressure-amorphization of hexagonal ice to HDA at 77 K.

Introduction

The glass → liquid transition in the amorphous forms of ice is central to theories which aim to understand the anomalies in liquid water,[1] *e.g.*, the second critical point hypothesis[2] or the singularity-free hypothesis.[3] These hypotheses rest on the assumption that the two distinct amorphous states called high-density amorphous (HDA) and low-density amorphous (LDA) ice, which were first made by Mishima *et al.*,[4,5] turn on heating into two distinct liquid states called high-density liquid (HDL) and low-density liquid (LDL). Thus both HDA and LDA should experience on isobaric heating a glass → liquid transition. For LDA a glass → liquid transition has been reported first by Handa and Klug by adiabatic calorimetry,[6] with an onset temperature (T_g) at 124 K and an increase in heat capacity (Δc_p) of 0.7 J K^{-1} mol^{-1} for heating at 0.17 K min^{-1}. After some confusion regarding LDA's T_g by differential scanning calorimetry (DSC) (see footnote† for details), Salzmann *et al.*[7] reported the DSC scan of LDA, with a T_g of 135 ± 2 K and the same Δc_p of 0.7 J K^{-1} mol^{-1} for heating at 30 K min^{-1}. The observation of LDA's T_g is consistent with the report that LDA deforms under load and

behaves like a viscous liquid near 143 K.[9] However, there is also some indication that LDA shows crystal-like behaviour. Comparison of vibrational spectra and oxygen K-edge X-ray absorption spectra of LDA with ice,[10–12] an analysis of Gibbs free energies,[13] the absence of fast precursor dynamics in QENS experiments,[14] crystal-like features in inelastic scattering[15,16] and in the thermal conductivity[17,18] suggest that LDA is not a truly amorphous material (reviewed in ref. 19). This may be rationalized by considering that LDA is always produced *via* HDA by mechanical collapse of hexagonal ice upon applying pressure,[5,10] and so crystalline remnants, *e.g.*, distorted nanosized crystals,[20] may survive up to the LDA stage. Therefore, it is not yet fully clear whether or not LDA transforms on heating into LDL, and further experiments are important.

Here we show that LDA's calorimetric glass → liquid transition is reversible, that is, it can be thermally cycled between its glassy state below 137 K and its highly viscous liquid state at 149 K. To enable comparison, we demonstrate reversibility in the manner shown previously for hyperquenched glassy water (HGW)[21,22] and vapour-deposited amorphous ice (ASW),[23] by recording two successive DSC scans of the same sample through the glass transition region and by observation of the same T_g value. We note that Handa and Klug[6] in their study of heat capacity and glass transition behaviour of LDA had annealed two LDA samples, one at 129 K and the other at 130 K, before recording their heat capacity and observing an endothermic peak with T_g of 124 K (see Fig. 1 and 2 in ref. 6, and the curves labelled "lda (129 K)" and "lda (130 K)"). Thus, irreversible relaxation effects have probably been

---

[a] Institute of Physical Chemistry, University of Innsbruck, Innrain 52a, A-6020 Innsbruck, Austria. E-mail: thomas.loerting@uibk.ac.at
[b] Institute of General, Inorganic and Theoretical Chemistry, University of Innsbruck, Innrain 52a, A-6020 Innsbruck, Austria
† We emphasize that our previous report of LDA's T_g of 129 K on heating at 30 K min^{-1} had been withdrawn because this endothermic feature had been caused by proton-order → disorder transition in ice XII which had formed besides HDA on pressure-amorphization of hexagonal ice (ice Ih). Details are given in ref. 7 and 8.

excluded by their annealing above their T_g, but reversibility as shown for HGW and ASW in the manner described above has not been established so far. We also report the glass → liquid transition and crystallization of D_2O LDA and show that the H/D isotope effect is remarkably similar to that of HGW.[24]

We further find that the preparation route of LDA makes a crucial difference. Until now both studies of LDA's T_g,[6,7] used LDA made in the same manner reported first by Mishima et al.,[5] by isobaric heating of HDA, which had been formed on pressure-amorphization of ice Ih at 77 K.[4] This HDA has been called u-HDA (for unrelaxed HDA) by Nelmes et al.[25] We
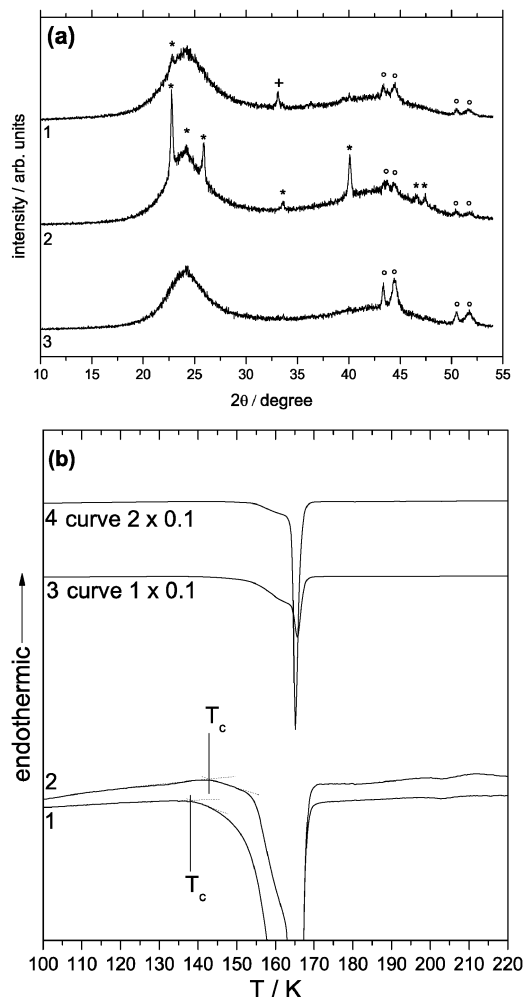
Fig. 1 (a) X-Ray diffractograms (Cu Kα₁) of one LDA_I and one LDA_II sample quenched and recovered at 77 K after thermal treatment, and recorded at 80 K. (1) LDA_I obtained from HDA (made by pressurizing ice Ih at 100 K to 1.6 GPa) by isobaric heating up to 138 K at 0.004 GPa, (2) LDA_I heated in addition up to 149 K at 0.006 GPa, and (3) LDA_II obtained from VHDA by isothermal decompression at 140 K to 0.006 GPa at a rate of 12 MPa min⁻¹, and heated subsequently to 149 K at 0.006 GPa. Bragg peaks from ice Ih are marked by asterisks, from the sample holder by a circle, and from a trace of indium by a cross. (b) DSC scans of one LDA_I and one LDA_II sample obtained on heating at 10 K min⁻¹. Curve 1 is the DSC scan of a LDA_I sample and curve 2 the scan of a LDA_II sample, both shown enlarged. The beginning of crystallization (marked by T_c) is in curve 1 at ≈138 K and in curve 2 at ≈143 K. Curves 3 and 4 are curves 1 and 2 shown on a reduced scale (1/10th).
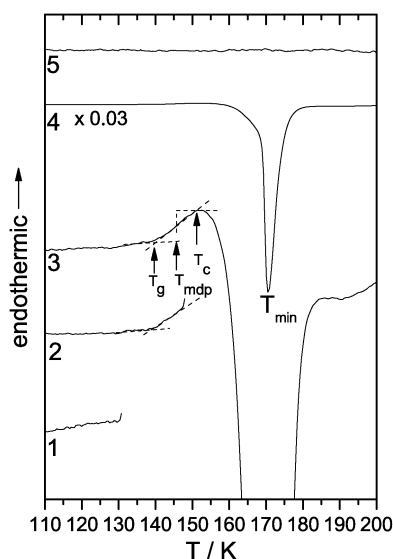
Fig. 2 Reversibility of the glass → liquid transition of H_2O LDA_II as seen in DSC scans. The same sample of 5.04 mg was used and it was heated or cooled with a rate of 30 K min⁻¹. Scan (1) was obtained on first heating to 131 K, scan (2) on second heating to 148 K (after annealing the sample at 131 K for 90 min and cooling to 93 K). Scan (3) was obtained on third heating to 210 K (after annealing the sample again at 131 K for 90 min and cooling to 93 K), scan (4) is scan (3) plotted on a reduced (1/30th scale) to show the full exotherm from crystallization to H_2O cubic ice. Scan (5) was obtained on fourth heating (after cooling the sample from 210 K to 93 K). For Fig. 2 and 3: T_g and Δc_p were evaluated as shown in scan (3) by dashed lines. Scans (1) to (3) and (5) are drawn on the same scale, but shifted for clarity. The temperature scale is not corrected for the thermal lag of the instrument.

recently reported two distinct structural states in LDA caused by relaxation effects and observed by neutron diffraction.[26] One, labelled LDA_I, is obtained by isobaric annealing of HDA close to ambient pressure,[4] the other, called LDA_II, is obtained by isothermal decompression of very high density amorphous ice (VHDA)[27] at 140 K from 1.1 to 0.006 GPa.[26,28,29] LDA_I and LDA_II are not distinct forms "in the way that LDA, HDA, and VHDA differ, but rather are two closely related, but kinetically trapped forms of what could be considered the true metastable low density amorphous ice",[26] and they differ on intermediate length scales in the hydrogen bonded water network, but not in density. In the course of this study we noticed that LDA_II is more stable towards crystallization than LDA_I: LDA_II can be repeatedly cycled in the DSC between 90 and 149 K without formation of crystalline ice, whereas for LDA_I slow formation of ice occurs on repeated cycling. Because of that, we use in our DSC study only LDA_II.

Experimental

The samples were pressurized and decompressed in a pressure vessel with 10 mm bore, by using a computerized universal testing machine (Zwick, model BZ100/TL3S). The sample volume is 300 μl of deionized water. Indium linings were used to avoid pressure drops during compression followed by shockwave heating and formation of ice XII.[28,30–33]
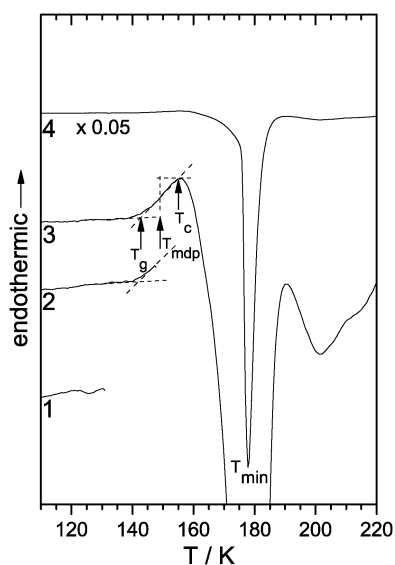
This journal is © the Owner Societies 2010

Phys. Chem. Chem. Phys., 2010, **12**, 708–712 | 709

Fig. 3 Isotope effect on the glass → liquid transition and crystallization as seen in DSC scans of D_2O LDA_{II}. The same sample of 8.03 mg was used and it was heated or cooled at a rate of 30 K min^{-1}. Scan (1) was obtained on first heating to 131 K, scan (2) on second heating to 148 K (after annealing the sample at 131 K for 90 min and cooling to 93 K). Scan (3) was obtained on third heating to 210 K (after annealing the sample again at 131 K for 90 min and cooling to 93 K), scan (4) is scan (3) plotted on a reduced (1/20th scale) to show the full exotherm from crystallization to D_2O cubic ice.

VHDA was made by heating HDA at 1.1 GPa to 160 K at ∼3 K min^{-1}.[27]

X-Ray diffractograms were recorded in θ–2θ geometry on a Siemens D5000 diffractometer, equipped with a low-temperature camera from Paar. The θ–θ arrangement of the instrument allowed to keep the sample in a horizontal position throughout the experiment. The instrument is equipped with a "Goebel mirror", providing monochromatic Cu Kα_1 radiation. This setup provides high intensity, stability of peak positions, and low background.

A differential scanning calorimeter (model DSC 4, Perkin Elmer) with a self-written computer program was used. A base line was recorded by heating the sample subsequently to 253 K, and it was subtracted from the scans (see ref. 34 for details). The sample was transferred under liquid N$_2$ into a stainless steel capsule with a screwable lid. The mass of the sample was obtained *via* the melting endotherm of ice, by using the value of 6.012 kJ mol^{-1} as heat of melting for H_2O ice, and of 6.280 kJ mol^{-1} for D_2O ice. LDA_{II} was made for DSC measurements by isothermal decompression of VHDA at 140 K from 1.1 to 0.006 GPa at a controlled rate of 12 MPa min^{-1}, and thereafter cooled to 77 K and quench-recovered under liquid nitrogen. The quench-recovered H_2O and D_2O LDA_{II} samples were controlled by X-ray diffraction and found to be fully amorphous. The DSC instrument was calibrated with cyclopentane.[35] For the heats of transition crimp-sealed Al pans were used to avoid evaporation losses. For determining thermal lag on heating at 30 K min^{-1}, cyclopentane in a stainless steel capsule (≈620 mg weight) was used, and *via* the onset temperature of its phase transition at 122.4 K,[35]

thermal lag was determined to be −1.8 K. Thermal lag is negligible on heating at 10 K min^{-1}.

Results and discussion

Enhanced stability of LDA_{II} towards crystallization is demonstrated in Fig. 1a by X-ray diffractograms. LDA_I develops on heating to 149 K at 0.006 GPa intense Bragg peaks of textured ice Ih (scan 1 *versus* scan 2), whereas LDA_{II} is still fully amorphous after heating to 149 K at 0.006 GPa (scan 3). In all three scans peak position of first broad peak is at $2\theta = 24.2°$, and thus LDA_I and LDA_{II} cannot be distinguished by routine X-ray diffractograms. Formation of ice Ih after partial crystallization of LDA_I (scan 2) instead of ice Ic seems surprising, but formation of ice Ih from HDA under pressure was also reported by Salzmann *et al.* (*cf.* Table 1 in ref. 36). We emphasize that the ice Ih Bragg peaks in curve 2 are not caused by ice Ih formed by condensation of water vapour during handling and transfer of the sample onto the precooled X-ray sample holder because we know from many experiments that this procedure is now routine and condensation of water vapour can be avoided. In addition, we observed intense texture effects such as those in curve 2 only when ice Ih formed from amorphous ice under pressure, and not in ice Ih formed by condensation of water vapour (see, *e.g.*, Fig. 1b in ref. 37). DSC scans of one LDA_I and one LDA_{II} sample shown in Fig. 1b are further consistent with enhanced propensity in LDA_I toward crystallization. Curve 1 is the DSC scan of a LDA_I sample and curve 2 the scan of a LDA_{II} sample, both shown enlarged. The beginning of crystallization (marked by T_c) is in curve 1 at ≈138 K and in curve 2 at ≈143 K, and thus T_c is shifted in LDA_{II} by ≈5 K to higher temperature in comparison to T_c of LDA_I. Curves 3 and 4 are curves 1 and 2 shown on a reduced scale (1/10th), and these curves demonstrate that the peak minimum temperatures are about the same.

The reversibility of the calorimetric glass → liquid transition features of H_2O LDA_{II} is demonstrated in Fig. 2. Scan (1) was recorded on first heating to 131 K. For scan (2) the sample was first annealed at 131 K for 90 min, cooled and then heated to 148 K at a rate of 30 K min^{-1}. The beginning of the glass transition endotherm is indicated by the change of slope at 139 K. The sample was thereafter cooled to 93 K, annealed again at 131 K for 90 min, cooled to 93 K, and then heated to 210 K and its DSC scan recorded as scan (3). The change of slope occurs at the same temperature of 139 K as in scan (2) which demonstrates its reversibility. Scan (4) is scan (3) plotted on a reduced (1/30th) scale to show the intense exotherm due to crystallization to ice Ic. T_g and T_{mdp} are onset and midpoint temperatures of the glass transition endotherm, and T_c and T_{min} mark the onset and minimum temperature of the strong exotherm due to crystallization to ice Ic. After correction for the thermal lag of the instrument, the values are 137 and 143 K for T_g and T_{mdp}, and 149 and 169 K for T_c and T_{min}. The increase in heat capacity in the glass transition region (Δc_p) was determined as shown in scan (3) by dashed lines, and is about 1.7 J K^{-1} mol^{-1}. The apparent width of the glass transition is 12 K. The heat of crystallization to ice Ic is −1.30 kJ mol^{-1}. Scan (5) is the scan of ice Ic formed in scan (3)

by heating to 210 K. The absence of the glass transition endotherm ensures that the endotherm is not caused by the DSC instrument.

The H/D isotope effect on the glass transition and crystallization of D_2O LDA_{II} is shown in Fig. 3. Scan (1) was recorded on first heating to 131 K. For scan (2) the sample was first annealed at 131 K for 90 min, cooled and then heated to 148 K at a rate of 30 K min^{-1}. The beginning of the glass transition endotherm is indicated by the change of slope at about 142 K. The sample was thereafter cooled to 93 K, annealed again at 131 K for 90 min, cooled to 93 K, and then heated to 210 K and its DSC scan recorded as scan (3). The change of slope occurs at the same temperature of 142 K as in scan (2) which demonstrates its reversibility. Scan (4) is scan (3) plotted on a reduced (1/20th) scale to show the intense exotherm due to crystallization to D_2O cubic ice. After correction for the thermal lag of the instrument, the values for T_g and T_{mdp} are 140 and 147 K, and for T_c and T_{min} 154 and 176 K. The increase of heat capacity in the glass transition region (Δc_p) was determined as shown in scan (3) by dashed lines, and is about 1.5 J K^{-1} mol^{-1}. The apparent width is 14 K. The heat of crystallization to D_2O ice Ic is -1.22 kJ mol^{-1}.

The reversibility of the glass → liquid transition endotherm established in this study for both H_2O and D_2O LDA_{II} shows that it can be thermally cycled between its glassy state below 137 K (140 K for D_2O), and its highly viscous liquid state at 148 K. This means that the structural states of glassy LDA_{II} and of highly viscous liquid water are thermodynamically continuous in the glass → liquid transition range. Furthermore, irreversible relaxation effects can be excluded as a cause of LDA's endothermic feature at T_g.

We next compare the glass → liquid transition features of LDA_{II} (H_2O and D_2O) with those of hyperquenched glassy water (HGW).[21,22,24,34,38] To make this comparison meaningful, the same heating and cooling rate of 30 K min^{-1} and the same annealing conditions were used for this study of LDA_{II} as for the previous ones of HGW. We find that the glass → liquid transition features of annealed LDA_{II} are remarkably similar to those of annealed HGW with respect to T_g, Δc_p, width and H/D isotope effect (see Table 1 in ref. 24 for thermal effects on reheating H_2O and D_2O HGW). Even the effect of isotopic substitution, observed first for H_2O and D_2O HGW, where T_g increases on deuteration much less than T_c, and so the width increases from ≈12 K to ≈15 K (see Table 1 in ref. 24) is observable for LDA_{II}, although to a slightly lesser extent (from ≈12 K to ≈14 K). Thus T_g and T_c become more separated in both D_2O HGW and LDA_{II} and the width of the glass transition region increases in comparison to the H_2O samples. This unexpected isotope effect is discussed for HGW in detail in ref. 24 and need not be repeated here. We conclude that LDA_{II} and HGW are highly similar states which are thermodynamically connected by heating to the same highly viscous liquid state.

The structural relaxation time, τ_s, calculated from a DSC scan obtained by heating at a rate of 30 K min^{-1} has been revised from ≈70 s at T_g,[39] to ≈33 s by considering both the non-exponentiality of structural relaxation and the structure dependence of τ_s.[40,41] Johari[41] determined the dielectric relaxation time, τ, of ultraviscous bulk water by analyzing

its loss tangent data, which had been obtained in earlier studies on heating ASW[42] and HGW.[43] He concludes that τ at 136 ± 1 K is 42 ± 14 s "when a distribution of relaxation times, a characteristic of viscous liquids, is assumed".[41] This value for τ agrees nicely with τ_s of ≈33 s estimated for T_g from the DSC endotherm on heating at 30 K min^{-1}. Johari concludes that "water is an ultraviscous liquid of viscosity of the order of 10^{12} poise at 136 K, and remains a viscous liquid until it crystallizes to cubic ice".[40] The same holds for H_2O (D_2O) LDA_{II} with a T_g of 137 (140) K, and so we consider it justified to describe the state of LDA_{II} above its T_g as that of a highly viscous liquid. This is further consistent with the report that LDA deforms under load and behaves like a viscous liquid near 143 K.[9]

For both HGW and LDA_{II}, the weak endothermic increase in c_p is followed by the intense exothermic feature from the beginning of crystallization to ice Ic, and this exotherm masks the c_p curve of the deeply supercooled liquid following the glass → liquid transition which is observable in less rapidly crystallizing glasses. The apparent peak of the T_g endotherm is therefore an artefact from superposition of the crystallization exotherm and the glass-softening endotherm. Thus, the end temperature of LDA's (and HGW's) glass → liquid transition and the c_p value at this temperature are not directly observable.[34]

The remarkable similarity between the glass → liquid transition features of LDA_{II} and HGW has implications for claims to reassign HGW's T_g to higher temperatures. First, Velikov et al. demand that HGW's T_g should be reassigned from 136 K to 165 ± 5 K.[44] Their claim is based on the intense enthalpy relaxation exotherm observed on reheating HGW, and the magnitude of the unrelaxed enthalpy remaining when crystallization occurred.[38] Their argument does not hold for LDA_{II} because an intense exotherm is not observable even on first heating (see scans 1 in Fig. 2 and 3). Second, Yue and Angell[45] compare HGW's glass transition behaviour with that of other inorganic hyperquenched glasses and conclude that "small endothermic effects, such as the one attributed to the glass transition of water, are only a "shadow" of the real glass transition occurring at higher temperatures, and that the glass transition of water cannot be probed directly". Since LDA_{II} has not been made by hyperquenching, an interpretation as a "shadow transition" is not possible. Later on, it was clarified that T_g for HGW can remain at 136 K, provided water experiences a fragile-to-strong transition upon cooling and behaves as an almost ideally strong liquid at 148 K,[46–48] which is consistent with our data.

In conclusion, the calorimetric features of both H_2O and D_2O LDA_{II} are fully consistent with a reversible glass → liquid transition, and these features and the effect of isotopic substitution are about the same as those observed for HGW. We thus need to discuss what causes the above-mentioned crystal-like behaviour of LDA in the studies of ref. 10–18. These studies have all been made with LDA formed on isobaric heating of HDA, what we now call LDA_I. We had attributed above the enhanced propensity of LDA_I towards crystallization to crystalline remnants, e.g., distorted nanosized crystals, which are still present in unrelaxed HDA after pressure-amorphization of ice Ih, and which can act as seeds for formation of cubic and/or hexagonal ice. In this context it

This journal is © the Owner Societies 2010

Phys. Chem. Chem. Phys., 2010, **12**, 708–712 | 711

is interesting to note that in the two previous calorimetric studies of annealed LDA$_I$,[6,7] Δc_p was observed to be only about half the value (0.7 J K^{-1} mol^{-1}) reported here for LDA$_{II}$. This lower value could be caused by a considerable amount of crystalline remnants in LDA$_I$. The enhanced stability of LDA$_{II}$ toward crystallization (see Fig. 1, curve (2) *versus* curve (3)) could be caused by the disappearance of such crystalline remnants during formation of VHDA at 1.1 GPa and 160 K. This is consistent with Klotz *et al.*'s[49] conclusion from *in situ* neutron diffraction studies of high-density amorphous ice under pressure that possible crystal-like grain size has to be below ≈ 2 nm and therefore VHDA has to be amorphous. Measurements of the dielectric relaxation time of HDA under pressure obtained from VHDA[20,50] give at 1 GPa a relaxation time of a few seconds at 130 K. This is consistent with HDA at 1 GPa being a highly viscous liquid in which crystalline remnants can be removed (*e.g.*, dissolve). It might seem surprising that such crystalline remnants do not induce further crystallization, as pointed out by one of the reviewers. However, at 1 GPa and 140 K we are in the stability field of ice VI,[51] and it is not at all clear to us whether crystalline remnants from hexagonal ice can act as nuclei for crystallization of stable ice VI. We conclude that it is possible that crystal-like behaviour of LDA$_I$ in ref. 10–18 is caused by crystalline remnants, *e.g.*, distorted nanosized crystals. We therefore suggest to repeat these measurements with samples of LDA$_{II}$ prepared in the manner reported here.

Acknowledgements

References

1 P. G. Debenedetti, *J. Phys.: Condens. Matter*, 2003, **15**, R1669.
2 P. H. Poole, F. Sciortino, U. Essmann and H. E. Stanley, *Nature*, 1992, **360**, 324.
3 S. Sastry, P. G. Debenedetti, F. Sciortino and H. E. Stanley, *Phys. Rev. E: Stat. Phys., Plasmas, Fluids, Relat. Interdiscip. Top.*, 1996, **53**, 6144.
4 O. Mishima, L. D. Calvert and E. Whalley, *Nature*, 1984, **310**, 393.
5 O. Mishima, L. D. Calvert and E. Whalley, *Nature*, 1985, **314**, 76.
6 Y. P. Handa and D. D. Klug, *J. Phys. Chem.*, 1988, **92**, 3323.
7 C. G. Salzmann, I. Kohl, T. Loerting, E. Mayer and A. Hallbrucker, *Phys. Chem. Chem. Phys.*, 2003, **5**, 3507.
8 C. G. Salzmann, P. G. Radaelli, J. L. Finney and E. Mayer, *Phys. Chem. Chem. Phys.*, 2008, **10**, 6313.
9 G. P. Johari, *J. Phys. Chem. B*, 1998, **102**, 4711.
10 J. S. Tse, D. D. Klug, C. A. Tulk, I. Swainson, E. C. Svensson, C. K. Loong, V. Shpakov, V. R. Belosludov, R. V. Belosludov and Y. Kawazoe, *Nature*, 1999, **400**, 647.
11 J. S. Tse, D. M. Shaw, D. D. Klug, S. Patchkovskii, G. Vankó, G. Monaco and M. Krisch, *Phys. Rev. Lett.*, 2008, **100**, 095502.
12 J. C. Li and P. Jenniskens, *Planet. Space Sci.*, 1997, **45**, 469.
13 G. P. Johari, *J. Chem. Phys.*, 2000, **113**, 10412.
14 B. Geil, M. M. Koza, F. Fujara, H. Schober and F. Natali, *Phys. Chem. Chem. Phys.*, 2004, **6**, 677.
15 D. D. Klug, C. A. Tulk, E. C. Svensson and C. K. Loong, *Phys. Rev. Lett.*, 1999, **83**, 2584.
16 H. Schober, M. M. Koza, A. Tolle, C. Masciovecchio, F. Sette and F. Fujara, *Phys. Rev. Lett.*, 2000, **85**, 4100.
17 O. Andersson and H. Suga, *Phys. Rev. B: Condens. Matter Mater. Phys.*, 2002, **65**, 140201.
18 O. Andersson and A. Inaba, *Phys. Chem. Chem. Phys.*, 2005, **7**, 1441.
19 T. Loerting, V. V. Brazhkin and T. Morishita, in *Advances in Chemical Physics*, ed. S. A. Rice, Wiley, Hoboken, NJ, 2009, vol. 143, p. 53.
20 O. Andersson, *J. Phys.: Condens. Matter*, 2008, **20**, 244115.
21 G. P. Johari, A. Hallbrucker and E. Mayer, *Nature*, 1987, **330**, 552.
22 A. Hallbrucker, E. Mayer and G. P. Johari, *Philos. Mag. B*, 1989, **60**, 179.
23 A. Hallbrucker, E. Mayer and G. P. Johari, *J. Phys. Chem.*, 1989, **93**, 4986.
24 G. P. Johari, A. Hallbrucker and E. Mayer, *J. Chem. Phys.*, 1990, **92**, 6742.
25 R. J. Nelmes, J. S. Loveday, T. Straessle, C. L. Bull, M. Guthrie, G. Hamel and S. Klotz, *Nat. Phys.*, 2006, **2**, 414.
26 K. Winkel, D. T. Bowron, T. Loerting, E. Mayer and J. L. Finney, *J. Chem. Phys.*, 2009, **130**, 204502.
27 T. Loerting, C. Salzmann, I. Kohl, E. Mayer and A. Hallbrucker, *Phys. Chem. Chem. Phys.*, 2001, **3**, 5355.
28 K. Winkel, M. S. Elsaesser, E. Mayer and T. Loerting, *J. Chem. Phys.*, 2008, **128**, 044510/1.
29 K. Winkel, M. S. Elsaesser, M. Seidl, M. Bauer, E. Mayer and T. Loerting, *J. Phys.: Condens. Matter*, 2008, **20**, 494212.
30 I. Kohl, E. Mayer and A. Hallbrucker, *Phys. Chem. Chem. Phys.*, 2001, **3**, 602.
31 M. Koza, H. Schober, A. Tölle, F. Fujara and T. Hansen, *Nature*, 1999, **397**, 660.
32 M. M. Koza, H. Schober, T. Hansen, A. Tölle and F. Fujara, *Phys. Rev. Lett.*, 2000, **84**, 4112.
33 T. Loerting, I. Kohl, C. Salzmann, E. Mayer and A. Hallbrucker, *J. Chem. Phys.*, 2002, **116**, 3171.
34 I. Kohl, L. Bachmann, A. Hallbrucker, E. Mayer and T. Loerting, *Phys. Chem. Chem. Phys.*, 2005, **7**, 3210.
35 J. G. Aston, H. L. Fink and S. C. Schumann, *J. Am. Chem. Soc.*, 1943, **65**, 341.
36 C. G. Salzmann, E. Mayer and A. Hallbrucker, *Phys. Chem. Chem. Phys.*, 2004, **6**, 5156.
37 C. G. Salzmann, I. Kohl, T. Loerting, E. Mayer and A. Hallbrucker, *J. Phys. Chem. B*, 2003, **107**, 2802.
38 I. Kohl, L. Bachmann, E. Mayer, A. Hallbrucker and T. Loerting, *Nature*, 2005, **435**, E1.
39 C. A. Angell and L. M. Torrell, *J. Chem. Phys.*, 1983, **78**, 937.
40 G. P. Johari, *Phys. Chem. Chem. Phys.*, 2005, **7**, 1091.
41 G. P. Johari, *J. Chem. Phys.*, 2005, **122**, 144508.
42 G. P. Johari, A. Hallbrucker and E. Mayer, *J. Chem. Phys.*, 1991, **95**, 2955.
43 G. P. Johari, A. Hallbrucker and E. Mayer, *J. Chem. Phys.*, 1992, **97**, 5851.
44 V. Velikov, S. Borick and C. A. Angell, *Science*, 2001, **294**, 2335.
45 Y. Yue and C. A. Angell, *Nature*, 2004, **427**, 717.
46 C. A. Angell, *J. Phys.: Condens. Matter*, 2007, **19**, 205112/1.
47 C. A. Angell, *Science*, 2008, **319**, 582.
48 C. A. Angell, *MRS Bull.*, 2008, **33**, 544.
49 S. Klotz, T. Straessle, A. M. Saitta, G. Rousse, G. Hamel, R. J. Nelmes, J. S. Loveday and M. Guthrie, *J. Phys.: Condens. Matter*, 2005, **17**, S967.
50 O. Andersson and A. Inaba, *Phys. Rev. B: Condens. Matter Mater. Phys.*, 2006, **74**, 184201.
51 V. F. Petrenko and R. W. Whitworth, *Physics of Ice*, Oxford University Press, Oxford, 1999.